Jets and correlations in heavy-ion collisions

Jana Bielčíková[*]

Nuclear Physics Institute, The Czech Academy of Sciences, 250 68 Řež, Czech Republic
E-mail: jana.bielcikova@ujf.cas.cz

We report on recent findings on jet suppression and in-medium modification in heavy-ion collisions at ultra-relativistic energies at the CERN LHC and BNL RHIC, where hot and dense QCD matter is created. These results are accompanied by discussion on particle correlation studies with a focus on small collision systems where novel unexpected features in particle production give rise to long-range pseudorapidity particle correlations referred to as a ridge.

[*]Speaker.

1. Introduction

Collisions of heavy ions at high energies at the Large Hadron Collider (LHC) at CERN and Relativistic Heavy Ion Collider (RHIC) at Brookhaven National Laboratory (BNL) allow to study properties of strongly interacting ("QCD") matter under extreme conditions of large temperature and energy density which are above the expected thresholds for creation of a deconfined state of nuclear matter, the quark gluon plasma (QGP). QGP, if created, lives only for a very short time and its elusive characteristics require usage of various probes and measurements of different observables. Heavy quarks, quarkonia and jets, which are commonly referred to as hard probes, are created in the first moments after the collision and are therefore considered as key probes of the QGP properties. In this proceedings we review recent measurements of jet interaction with nuclear matter while an overview of heavy quark and quarkonia production is presented in [1].

Initial studies of jet interaction with QCD matter (*"jet quenching"*) at the center of mass energy per nucleon pair $\sqrt{s_{NN}} = 200$ GeV accessible at RHIC were based on measurements of inclusive particle production at large transverse momentum (p_T) [2–4] and dihadron azimuthal correlations with high-p_T trigger hadrons [5,6] which can be used as a proxy for jets. In these measurements the jet quenching effect manifested itself by a large suppression of high-p_T particle production by a factor of five relative to proton-proton (pp) collisions and disappearance of the away-side jet at intermediate $p_T = 2$–6 GeV/c compensated by increased production of low p_T particles. Dihadron correlations showed in addition a striking difference relative to pp collisions - a new extended correlation in pseudorapidity commonly referred to as the ridge which is present around the trigger particle at low and intermediate p_T of associated charged particles [7,8]. Measurements with leading hadrons are however known to suffer from several limitations. The leading hadrons are a mixture of parent quarks and gluons and as a fragmentation product carry only a part of original parton energy. In addition these measurements are influenced by a surface bias because leading hadrons predominantly originate from the surface of the asymmetric collision zone. Nevertheless even in the LHC era dihadron correlations remain a useful experimental observable that is complementary to fully reconstructed jets and that brought several puzzling observations including the observation of the ridge in high-multiplicity pp and p+Pb collisions in which no hot and dense QCD matter is formed and which we will discuss below.

Complete understanding of jet quenching requires inevitably measurements of reconstructed jets. However full jet reconstruction is a challenging task in the environment of heavy-ion collisions due to presence of large and fluctuating underlying background. Although pioneering measurements with reconstructed jets were already conducted at RHIC [9,10], the LHC measurements in Pb+Pb collisions at $\sqrt{s_{NN}} = 2.76$ TeV undoubtedly started a new era and intensive development of jet analysis and related correction methods. These jet measurements at the LHC renewed interest in jet analyses at RHIC where in the meantime large statistics data samples became available.

2. Dijet and correlated jet pair production

Run1 measurements of jet production in Pb+Pb collisions at the LHC energy of $\sqrt{s_{NN}} = 2.76$ TeV showed that inclusive jet [11–14] as well as dijet [15,16] production is significantly modified with respect to that in pp collisions. Inclusive jet production in central Pb+Pb collisions is suppressed
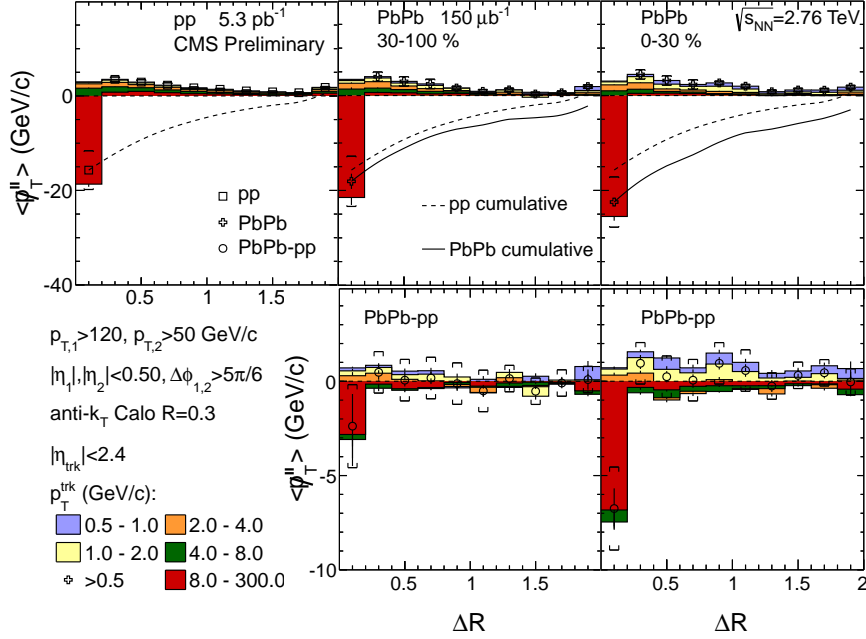
Figure 1: Top row: CMS measurement of differential $\displaystyle{\not}p_{\mathrm{T}}^{\parallel}$ distributions for pp, 30–100 % and 0–30 % Pb+Pb collisions at $\sqrt{s_{\mathrm{NN}}}$ = 2.76 TeV as a function of annulus radius ΔR. Various p_{T} ranges studied correspond to coloured boxes. The total $\displaystyle{\not}p_{\mathrm{T}}^{\parallel}$ integrated over all p_{T} in a given ΔR for pp (squares) and Pb+Pb (crosses) data is shown as well. Dashed and solid lines correpond to the cumulative $\displaystyle{\not}p_{\mathrm{T}}^{\parallel}$ distribution for pp and Pb+Pb data. Bottom row: Difference between the Pb+Pb and pp differential and total $\displaystyle{\not}p_{\mathrm{T}}^{\parallel}$ distributions. Figure from [18].

corroborating earlier findings of inclusive charged particle suppression at high p_{T}. In addition, the amount of the suppression varies with azimuthal angle of jet relative to the event plane [17] pointing to path length effects on the evolution of parton shower in the QCD matter. While inclusive jet measurements are sensitive to the average partonic energy loss, dijet measurements probe differences in the quenching between two parton showers traversing the medium. To quantify energy imbalance between the leading and sub-leading jet in a given event, the ATLAS experiment measured a dijet asymmetry A_{J} defined as [15]:

$$A_{\mathrm{J}} = \frac{E_{\mathrm{T}}^{\mathrm{lead}} - E_{\mathrm{T}}^{\mathrm{sublead}}}{E_{\mathrm{T}}^{\mathrm{lead}} + E_{\mathrm{T}}^{\mathrm{sublead}}}, \tag{2.1}$$

where $E_{\mathrm{T}}^{\mathrm{lead}}$ and $E_{\mathrm{T}}^{\mathrm{sublead}}$ is the transverse energy of the leading jet and the sub-leading jet in the opposite hemisphere defined as $|\Delta\phi| > \pi/2$ with $\Delta\phi$ being the azimuthal angle difference between the two jets, respectively. This early measurement of ATLAS followed shortly by CMS [16], showed a large enhancement of A_{J} in central relative to peripheral Pb+Pb collisions. In addition, CMS established that the large momentum imbalance is accompanied by a softening of the fragmentation pattern of the sub-leading jet. Consequently, A_{J} is recovered when integrating low p_{T} particles distributed over large angles relative to the direction of the sub-leading jet.

New studies of A_{J} with high statistics 2011 Pb+Pb data and measured pp reference in 2013 presented at the conference allow for a detailed investigation of the angular radiation pattern. The mul-
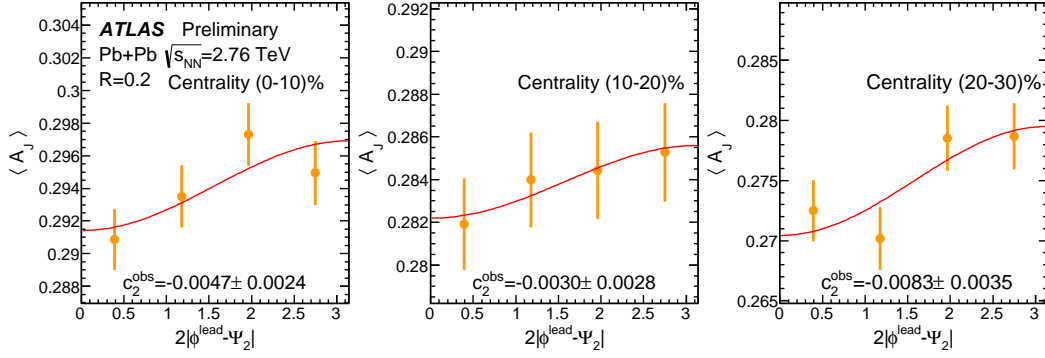
Figure 2: The ATLAS measurement of $\langle A_J \rangle$ as a function of azimuthal angle of leading jet relative to event plane together with fits to the second order Fourier harmonic term (c_2). Figure taken from [19].

tiplicity, angular and p_T spectra of the radiation balancing large A_J were characterized by CMS using several techniques as a function of the Pb+Pb collision centrality, A_J and dijet momentum [18]. It is found that for a given A_J, the dijet in-cone momentum imbalance (*missing p_T*)

$$\displaystyle{\not}p_T^{\parallel} = \sum_i -p_T^i \cos\left(\phi_i - \phi_{\text{Dijet}}\right)$$

(2.2)

is in Pb+Pb collisions compensated by particles with low $p_T = 0.5$–2.0 GeV/c, while in pp collisions by particles with larger momenta (2–8 GeV/c). This also leads to a larger associated particle multiplicity in Pb+Pb compared to pp data. The observed difference increases with Pb+Pb collision centrality. In Figure 1 is displayed a direct measurement of angular dependence of missing p_T up to large distances from the jet axis ($\Delta R = 1.8$). The angular pattern of the energy flow in Pb+Pb collisions is similar to that in pp, despite the large shift in the p_T spectrum of associated particles.

The ATLAS Collaboration presented at the conference dependence of the dijet asymmetry on the angle between the leading jet and the event plane angle [19]. Figure 2 shows this angular dependence for mean A_J in three different centrality bins of Pb+Pb collisions. The measured distributions are quantified by calculating the second Fourier coefficient c_2. Despite its very small magnitude ($|c_2| \approx 2\%$), the c_2 is systematically negative which indicates a slightly larger asymmetry for dijet pairs oriented perpendicular to the event plane. It would be very interesting to use this measurement in combination with non-zero single jet v_2 measurements [17, 20] and other jet observables discussed here and confront model calculations to provide simultaneous description of the experimental data and enable to constrain parton energy loss mechanism in medium.

Another differential measurement performed recently by ATLAS is study of the production of correlated jet pairs [21] which can be used to quantify fluctuations in the jet energy loss and help to discriminate among theoretical models. This correlated jet pair production is quantified by the rate of neighbouring jets $R_{\Delta R}$ that accompany a test jet within a given range of angular distance ΔR:

$$R_{\Delta R}(E_T^{\text{test}}, E_T^{\text{nbr}}) = \frac{\sum_{i=1}^{N_{\text{jet}}^{\text{test}}} N_{\text{jet},i}^{\text{nbr}}(E_T^{\text{test}}, E_T^{\text{nbr}}, \Delta R)}{N_{\text{jet}}^{\text{test}}(E_T^{\text{test}})},$$

(2.3)

where $E_T^{\text{test}}(E_T^{\text{nbr}})$ is the transverse energy of the test (nearby) jet, $N_{\text{jet}}^{\text{test}}$ is the number of test jets in a given E_T^{test} bin and $N_{\text{jet}}^{\text{nbr}}$ is the number of nearby jets. After subtraction of contribution from
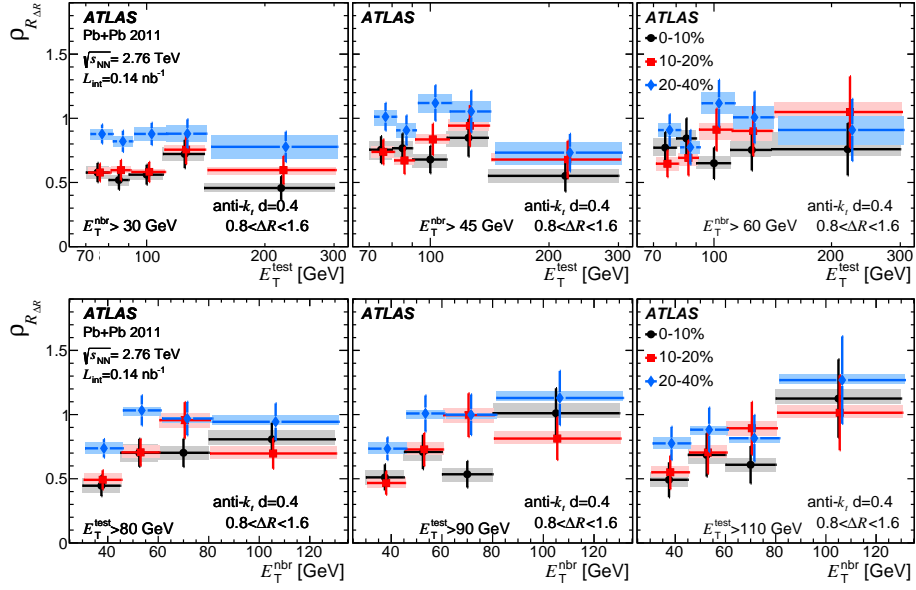
Figure 3: $\rho_{R_{\Delta R}}$ distributions in Pb+Pb collisions measured by ATLAS at $\sqrt{s_{\rm NN}} = 2.76$ TeV relative to 40–80% centrality as a function of jet energy [21]. Top (bottom) row: $\rho_{R_{\Delta R}}$ is evaluated as a function of $E_{\rm T}^{\rm test}$ ($E_{\rm T}^{\rm nbr}$) for three different choices of $E_{\rm T}^{\rm nbr}$ ($E_{\rm T}^{\rm test}$). The data points and horizontal uncertainties for individual centrality bins are shifted along the horizontal axis with respect to 0–10% centrality bin for clarity.

different hard scattering processes, remaining neighbouring jet pairs originate from the production of multiple jets in the same hard scattering process. A significant dependence of $R_{\Delta R}$ on collision centrality in Pb+Pb collisions was observed and further quantified using the central-to-peripheral ratio of $R_{\Delta R}$ distributions ($\rho_{R_{\Delta R}}$) displayed in Figure 3. The $\rho_{R_{\Delta R}}$ as a function of $E_{\rm T}^{\rm test}$ exhibits a suppression of 0.5–0.7 in 10% most central Pb+Pb collisions and does not show any strong dependence on $E_{\rm T}$. There are indications that suppression of $\rho_{R_{\Delta R}}$ as a function of nearby-jet $E_{\rm T}$ decreases with increasing nearby jet $E_{\rm T}$ but data have currently limited statistical significance.

3. h-jet correlation measurements

Measurements of jets recoiling from a hard trigger particle in A+A collisions offer a new unique approach to jet quenching studies. This study was introduced by ALICE [22] and followed by STAR [23, 24] although with a technically different implementation of the signal extraction. Both experiments analyze semi-inclusive differential distributions of charged jets recoiling from a charged trigger hadron with a transverse momentum $p_{T,trig}$ in a given interval ("TT"). Such distribution normalized by the number of trigger hadrons ($N_{\rm trig}^{\rm AA}$) can be written as:

$$\frac{1}{N_{\rm trig}^{\rm AA}} \frac{{\rm d}^2 N_{\rm jet}^{\rm AA}}{{\rm d}p_{\rm T,jet}^{\rm ch} {\rm d}\eta_{\rm jet}} \bigg|_{p_{\rm T,trig} \in {\rm TT}} = \left(\frac{1}{\sigma^{\rm AA \to h+X}} \cdot \frac{{\rm d}^2 \sigma^{\rm AA \to h+jet+X}}{{\rm d}p_{\rm T,jet}^{\rm ch} {\rm d}\eta_{\rm jet}} \right) \bigg|_{p_{\rm T,h} \in {\rm TT}}, \qquad (3.1)$$

where $\sigma^{\rm AA \to h+X}$ is the cross section to generate a hadron within the $p_{\rm T}$ interval of the TT class, ${\rm d}^2 \sigma^{\rm AA \to h+jet+X}/{\rm d}p_{\rm T,jet}^{\rm ch}{\rm d}\eta$ is the differential cross section for production of a hadron in the TT interval and a recoiling charged jet, and $p_{\rm T,jet}^{\rm ch}$ and $\eta_{\rm jet}$ are the charged jet transverse momentum
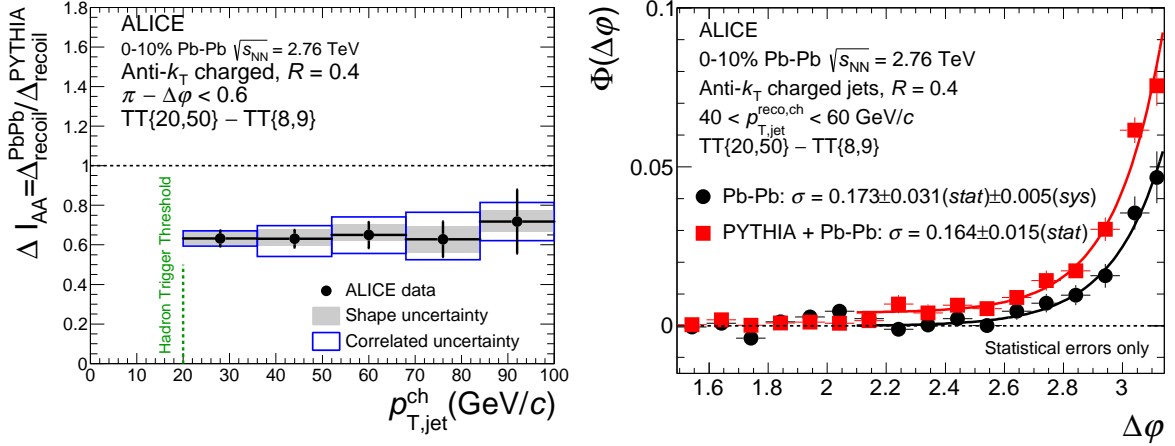
Figure 4: Left: the nuclear modification factor I_{AA} of recoiling jets in central Pb+Pb collisions at $\sqrt{s_{NN}}$ = 2.76 TeV measured by ALICE. Right: azimuthal distribution of recoiling jets relative to trigger hadron orientation in Pb+Pb (squares) data and PYTHIA (circles) together with a Gaussian fit (lines) [22].

and pseudorapidity, respectively. In order to remove background contributions, ALICE introduced a Δ_{recoil} observable defined as a difference of semi-inclusive recoil jet distributions from Eq. (3.1) for the signal (TT$_{Sig}$) and reference trigger particle (TT$_{Ref}$) classes as:

$$\Delta_{recoil} = \frac{1}{N_{trig}^{AA}} \frac{d^2 N_{jet}^{AA}}{dp_{T,jet}^{ch} d\eta_{jet}}\bigg|_{p_{T,trig} \in TT_{Sig}} - \frac{1}{N_{trig}^{AA}} \frac{d^2 N_{jet}^{AA}}{dp_{T,jet}^{ch} d\eta_{jet}}\bigg|_{p_{T,trig} \in TT_{Ref}}, \tag{3.2}$$

with the signal class TT$_{Sig}$ having higher p_T trigger hadrons than the TT$_{Ref}$ class. The TT$_{Sig}$ class corresponds to scattering processes with larger momentum transfers (Q^2) and therefore the associated recoiling jets have a harder p_T spectrum than those from the TT$_{Ref}$ class. The positive part of the recoiling jet spectra is however in both classes populated by random matching of the trigger hadron and background jets. STAR uses a mixed event technique to subtract the uncorrelated combinatorial background in the signal TT$_{Sig}$ distribution described in [23, 24]. By this procedure a fully uncorrelated sample of charged tracks is created preserving essential features of the measured events. Such mixed event (*ME*) distribution is then subtracted from that in real events (*SE*) with a trigger hadron chosen in a random direction and finally corrected for background fluctuations and instrumental effects using unfolding methods [25, 26]. The resulting spectra are divided by the reference pp spectra from PYTHIA in case of ALICE and peripheral Au+Au collisions in case of STAR due to the lack of measured pp reference in both experiments.

Figure 4 (left) shows the nuclear modification factor I_{AA} of the recoil charged jets in Pb+Pb collisions at $\sqrt{s_{NN}}$ = 2.76 TeV measured by ALICE for the resolution parameter $R = 0.4$ [22]. The data at the LHC energy shows a significant suppression of recoiling jet yield relative to pp reference by up to a factor two. This indicates that the in-medium energy loss arises predominantly from radiation at angles larger than 0.5. This suppression is even stronger in Au+Au collisions at RHIC ($\sqrt{s_{NN}}$ = 200 GeV) as demonstrated in Figure 5 (left), where together with the corrected recoil charged jet spectra in central and peripheral collisions for $R = 0.3$, also the central-to-peripheral ratio I_{CP} is shown. Despite a larger suppression of recoiling jet yields at RHIC energy, it is interesting to note that a similar horizontal shift of -8±2 GeV/c in the jet p_T spectrum to match peripheral
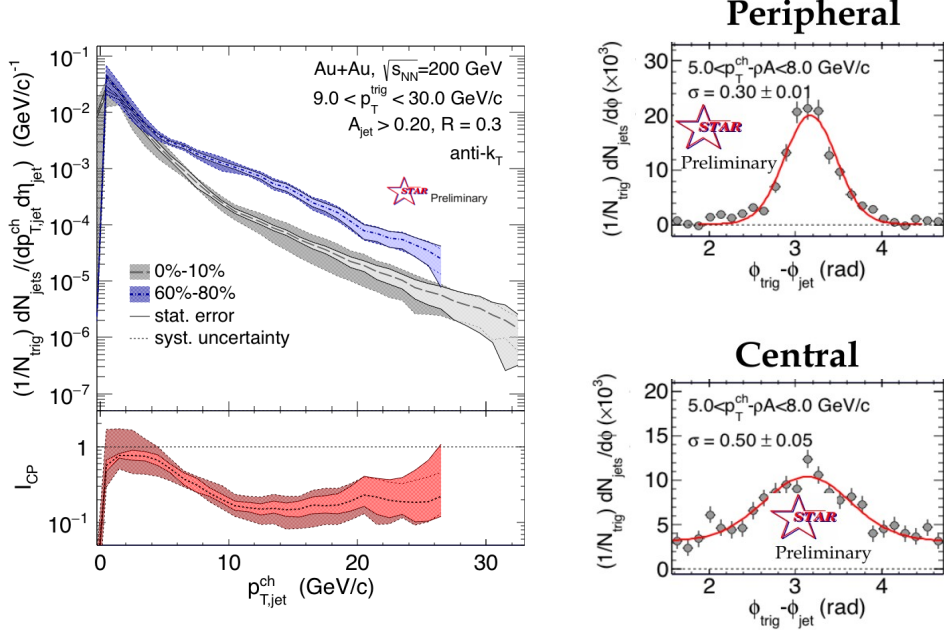
Figure 5: Left: Per trigger normalized recoil jet yield in central (0–10%) and peripheral (60–80%) Au+Au collisions at $\sqrt{s_{NN}} = 200$ GeV (top) and the central-to-peripheral ratio of the yield I_{CP} measured by the STAR experiment [24]. Right: Azimuthal distribution of trigger hadrons and recoiling charged jets ($p_T^{jet} = 5$–10 GeV/c) in peripheral (top) and central (bottom) Au+Au collisions [23].

(PYTHIA) to central A+A collision spectra is needed. This indicates that the larger suppression of recoiling jets at RHIC arises from similar out-of-cone radiation in combination with a steeper underlying jet spectrum relative to LHC energy. We would like to note that both measurements could however suffer from different surface bias which needs to be investigated in more detail.

To further explore nature of jet quenching, one can study the deflection of the recoil jet axis relative to the signal trigger hadron by replacing the jet p_T by an azimuthal angle difference $\Delta(\phi)$ in Eq. (3.1). At the LHC the azimuthal distributions of jets with $p_T = 40$–60 GeV/c do not show any significant medium-induced acoplanarity (cf. Figure 4 (right)) in agreement with direct photon-jet [27] and dijet correlation studies discussed above. While the same is also true at RHIC for the higher TT_{Ref} range of 9–30 GeV/c and recoil jets with $p_T = 8$–12 and 12–32 GeV/c, for jets with lower momenta ($p_T = 5$–8 GeV/c) a strong acoplanarity is observed as demonstrated in Figure 5 (right). Not only the amount of the acoplanarity is important but the rate of large angular deviations in tails of the $\Delta\phi$ distribution is sensitive to the quasi-particle nature of the medium and is expected to arise predominantly from single hard (Molière) scattering in the medium. A first study performed by ALICE in Pb+Pb collisions shows no evidence for Molière scattering [22], unfortunately statistical precision of this measurement is currently limited and requires more statistics which should become available in Run2 at the LHC.

4. Strange particle production in jets and bulk

Measurements of identified particle spectra in jets provide an important tool to understand interplay of various hadronization mechanisms in hot and dense medium. Already the first measurements at RHIC established that in heavy-ion collisions an increased production of baryons over
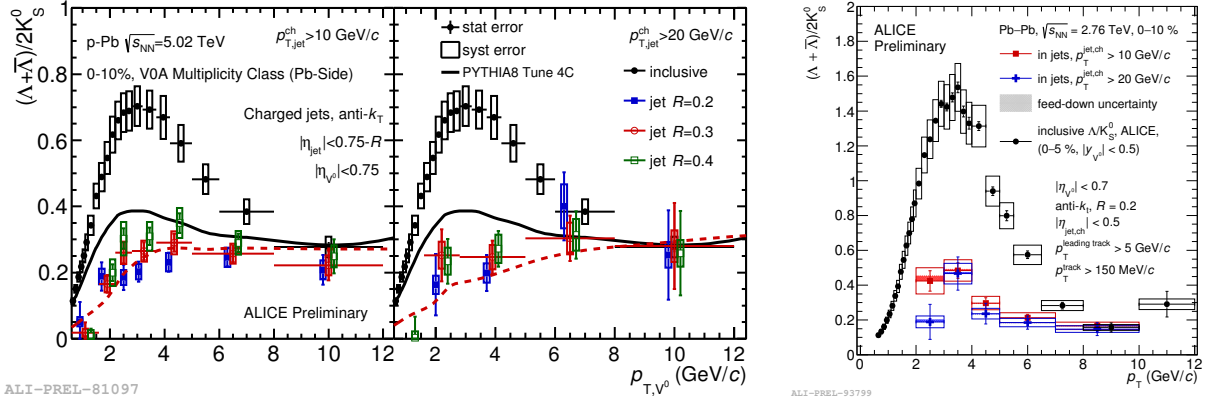
Figure 6: Λ/K_S^0 ratio associated with charged jets in p+Pb collisions at $\sqrt{s_{NN}}$ = 5.02 TeV (left) and Pb+Pb collisions at $\sqrt{s_{NN}}$ = 2.76 TeV (right) measured by ALICE [38, 39]. Black solid symbols correspond to inclusive Λ/K_S^0. Black solid line corresponds to inclusive ratio from PYTHIA8 simulation and the red dashed lines denote the spread of the ratio in PYTHIA8 jets for R = 0.2–0.4.

mesons relative to that in proton-proton collisions is present at intermediate transverse momenta (p_T = 2–6 GeV/c) [28–30]. This finding is also corroborated by recent studies in Pb+Pb collisions at the LHC [31], where in addition enhanced baryon/meson production in a small p+Pb collision system, although of a smaller magnitude, is present as well [32]. While this phenomenon obtained in last years lots of attention from theorists, a unique and fully satisfactory explanation is still missing. Currently among the preferred scenarios are an interplay of jet fragmentation (possibly modified by medium) with parton recombination and coalescence [33–35], hydrodynamically expanding bulk matter, jets, and the interaction between them [36] or radial flow effects [37]. Figure 6 displays first direct measurements of Λ/K_S^0 ratio associated with charged jets with p_T > 10 and 20 GeV/c in high-multiplicity p+Pb collisions at $\sqrt{s_{NN}}$ = 5.02 TeV [38] and 0–10% central Pb+Pb collisions at $\sqrt{s_{NN}}$ = 2.76 TeV from ALICE [39] together with the corresponding ratio of inclusively produced strange particles. In both collision systems the Λ/K_S^0 ratio associated with hard production is significantly below that measured in inclusive data and very similar to the ratio in pp collisions as demonstrated by comparing the data with PYTHIA simulations. Within the current experimental precision, the data is consistent with no medium modification of strange particle production in jets.

5. Collectivity in small systems: the ridge

Two-particle correlation studies are based on measurements of azimuthal ($\Delta\phi$) and pseudorapidity ($\Delta\eta$) angular differences between a *trigger* particle selected in a transverse momentum $p_{T,trig}$ interval and an (*associated*) particle that is detected with a lower transverse momentum, $p_{T,assoc}$. In pp collisions, the correlation at small angular differences ($\Delta\phi, \Delta\eta \approx 0$) and p_T > 2 GeV/c is naturally dominated by 'jet-like' correlations because both trigger and associated particles originate from the same fragmenting parton. These correlations then result in presence of a *near-side jet-like peak* in the $\Delta\phi \times \Delta\eta$ distributions. In contrast, at large azimuthal differences ($\Delta\phi \approx \pi$) no such pronounced peak is present because trigger and associated particles come from two different

colliding partons and an elongated pseudorapidity structure on the *away side* of the trigger particle is created. Below we focus on discussion of near-side peak properties due to limited space.

At RHIC energies it was discovered that the near-side peak is accompanied in heavy-ion collisions by a novel extended pseudorapidity correlation, the ridge [7, 8]. These findings were also later corroborated by measurements in Pb+Pb collisions at the LHC [40–42]. Although in small collision systems such as pp or p+A no dense QCD matter is expected to be formed, recent measurements at the LHC in pp collisions at $\sqrt{s}$ = 7 TeV [46] and p+Pb collisions at $\sqrt{s_{NN}}$ = 5.02 TeV [47–49] show that also there the near-side jet-like peak is accompanied by the ridge when events with particle multiplicity approaching that of peripheral A+A collisions are analyzed. In fact, after subtracting from the correlation distribution in high-multiplicity collisions that in low-multiplicity collisions, the remaining distribution reveals presence of the ridge-like correlations at both near and away side of the trigger particle.

To quantitatively describe properties of two-particle distributions, the distributions are commonly decomposed into a Fourier series of v_n coefficients with $n = 2$ (*elliptic*) and $n = 3$ (*triangular*) coefficients being the dominant contributions. The v_n coefficients are sensitive to the initial state geometry and can be associated with transport properties of the QCD matter in hydrodynamical models. The physics mechanism of the ridge in small collision systems could be however potentially different as the size of collision volume is smaller and the system may not be able to reach equilibrium and consequently hydrodynamical description will not be applicable. Several alterna-
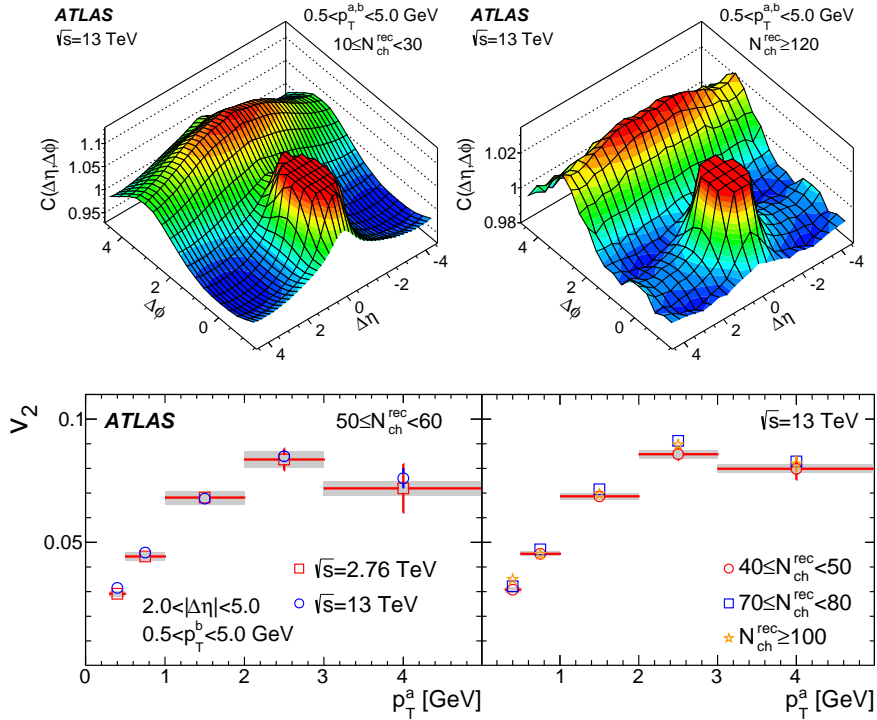
Figure 7: Top: Two-particle correlations at $\sqrt{s}$ = 13 TeV pp collisions measured by ATLAS [50] for charged particles with p_T = 0.5–5.0 GeV/c and $|\eta| < 4.6$ in two multiplicity intervals: 10–30 (left) and $\geq$ 120 (right). Bottom: v_2 values as a function of associated track p_T for 13 and 2.76 TeV pp data in the 50–60 multiplicity interval (left) and three different multiplicity intervals in the 13 TeV pp data (right).
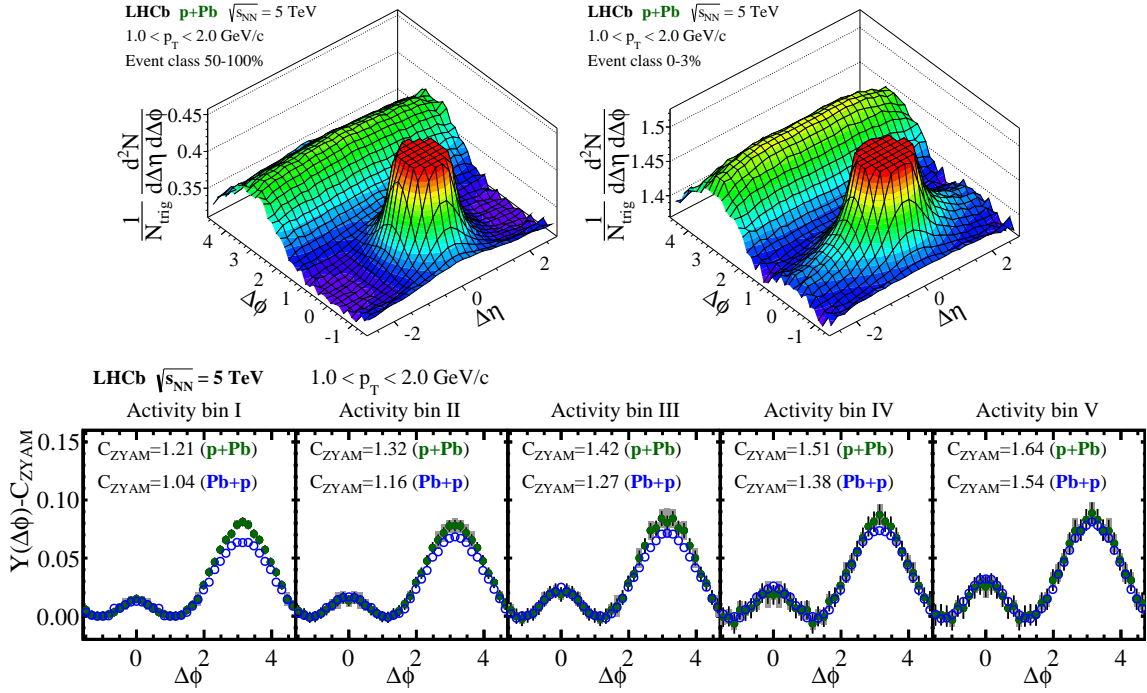
Figure 8: Two-particle correlations of charged particles with p_T = 1–2 GeV/c in p+Pb collisions at $\sqrt{s_{NN}}$ = 5.02 TeV measured by the LHCb experiment at forward rapidity. Top row: 2D correlations in low (left) and high (right) event-activity classes. Bottom row: 1D azimuthal correlations after the ZYAM background subtraction in $2.0 < \Delta\eta < 2.9$ in identical p+Pb and Pb+p event activities. Figures taken from [51].

tive theoretical models for ridge in small systems were proposed. Besides hydrodynamic effects in a high-density system [43, 44], an alternative model including gluon saturation in the incoming nucleons was shown to describe data as well [45]. On the experimental side intense effort has been carried in parallel to theoretical developments resulting in observations which clearly support collective origin of the ridge phenomenon in small systems and which we review below. At the conference ATLAS showed for the first time that the ridge persists also in $\sqrt{s}$ = 13 TeV high multiplicity collisions as shown in Figure 7 [50]. The extracted v_2 Fourier coefficient exhibits factorization characteristic of a global modulation of the per-event single-particle distributions and its magnitude at $\sqrt{s}$ = 2.76 and 13 TeV is within uncertainties the same suggesting that the physics mechanism does not have a strong collision energy dependence.

All these analyses were however performed in the central rapidity region, probing ranges of up to $|\Delta\eta| < 2.5$. At the conference, LHCb and ALICE presented extension of these studies to forward-forward and forward-backward rapidity regions, respectively. The unique forward acceptance layout of the LHCb detector among the LHC experiments offers to study the ridge in p+Pb collisions in the range of $2.0 < \eta < 4.9$ as shown in Figure 8 [51]. In the asymmetric LHCb detector layout, the ridge was separately confirmed for both p+Pb and Pb+p beam configurations which probe nucleon-nucleon c.m.s. rapidities of $1.5 < y < 4.4$ and $2.5 < y < 5.4$, respectively. The "forward" ridge is most pronounced in p_T = 1–2 GeV/c [51] and shows qualitatively similar features as that in central rapidity. When probing identical absolute activity ranges in the p+Pb and Pb+p configurations the strengths of the ridge are compatible with each other.
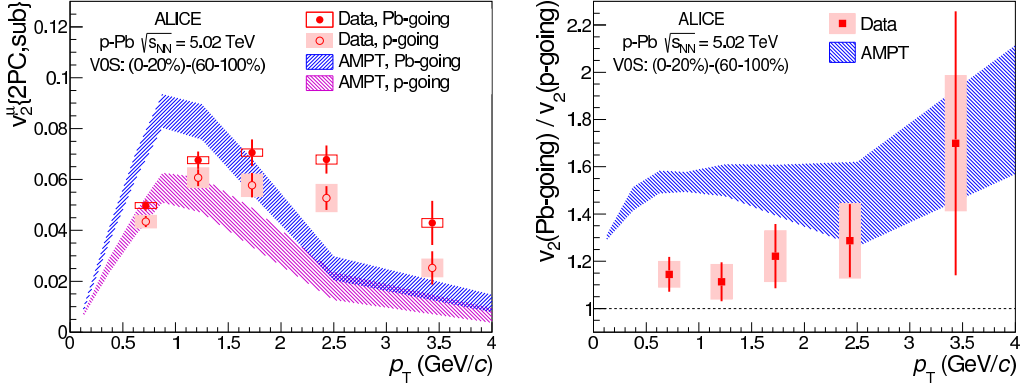
Figure 9: The elliptic anisotropy (v_2) values from muon-tracklet correlations in p-going and Pb-going directions (left) and their ratio (right) in p+Pb collisions at $\sqrt{s_{NN}}$ = 5.02 TeV for -4 < η < -2.5 measured by ALICE [52]. The data are compared to model calculations from AMPT [53].

ALICE measured forward-backward two-particle correlations utilizing muons from the muon tracker in the forward pseudorapidity range (2.5 < η < 4.0) as trigger particles and tracks measured by the central barrel detectors at midrapidity (η < 1.0) as associated particles [52]. This study which is presented in Figure 9 extended earlier studies at midrapidity [48, 49] and confirms that the double ridge structure persists to large pseudorapidity differences. The v_2 coefficients in high-multiplicity after subtracting jet-like correlations from low-multiplicity p+Pb events have a similar p_T dependence in p-going and Pb-going configurations, with the latter being by about 16±6% larger. Although the multi-phase transport model (AMPT) [53] predicts a different p_T and η dependence than observed in the data, we note that the results are sensitive to the parent particle v_2 and related composition of reconstructed muon tracks as the contribution from heavy flavour decays is expected to dominate at p_T > 2 GeV/c and should be reflected in any model comparison to draw quantitative conclusions.

In hydrodynamical models, the azimuthal anisotropies of particles produced in final state should depend on the particle mass and in the kinematic regime applicable for hydrodynamical description (p_T < 2 GeV/c) and consequently the anisotropy is predicted to be larger for lighter particles [37, 54]. The presence of such mass ordering was first established in Au+Au collisions at RHIC energies [55, 56] and later corroborated by measurements at the LHC [57] for light flavour hadrons containing u, d, and s quarks. The mass ordering has also been observed in small collision systems such as p+Pb [58] and d+Au [59] collisions for pions, kaons and protons consistent with expectations from hydrodynamical models [60, 61]. The CMS results presented at the conference [62] and published in [63] further extend our knowledge by measuring both anisotropies of neutral strange mesons (K_S^0) and baryons (Λ). The CMS data for elliptic (v_2) and triangular (v_3) anisotropy coefficients are shown in Figure 10. The data in high multiplicity p+Pb events show the anticipated mass ordering in $v_2(p_T)$ and $v_3(p_T)$ for p_T < 2 GeV/c with charged particles, composed mainly from pions, manifesting the smallest anisotropy followed by heavier K_S^0 mesons and eventually Λ baryons. It is interesting to note that for similar event multiplicities, the particle species dependence of v_2 and v_3 at low p_T is more pronounced in p+Pb than in Pb+Pb collisions which could be caused by a stronger radial flow boost in p+Pb collisions. The data are consistent with
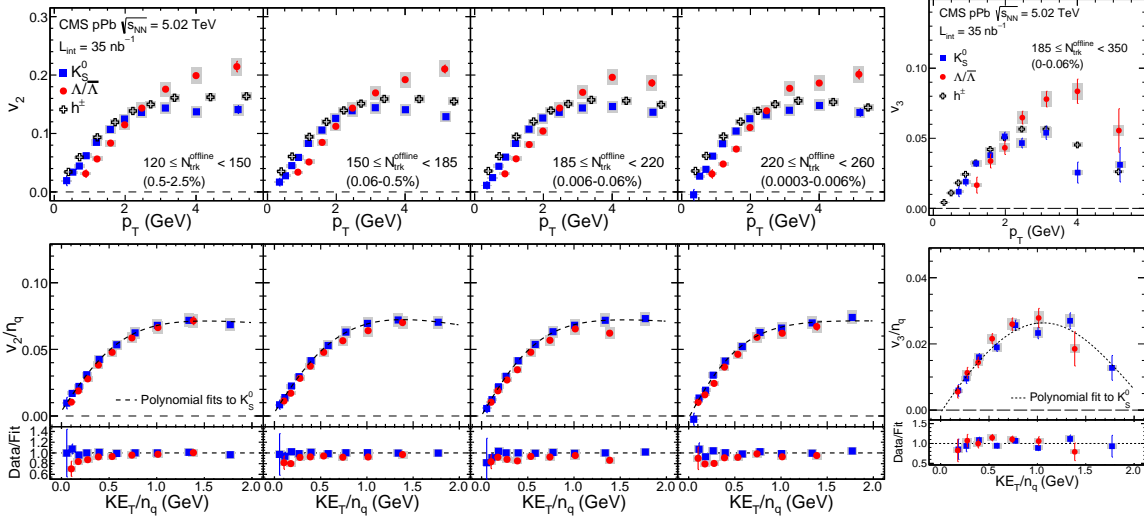
Figure 10: Top row: v_2 (left panel) and v_3 (right panel) values for K_S^0 (squares), $\Lambda/\bar{\Lambda}$ (circles) and charged particles (crosses) as a function of p_T in several p+Pb multiplicity at $\sqrt{s_{NN}} = 5.02$ TeV measured by CMS [63]. Bottom row: v_2 (v_3) values scaled by number of constituent quarks (n_q) as a function of transverse kinetic energy KE_T scaled by n_q together with a polynomial function fit for K_S^0 data.

quark number scaling at the level of 10% as demonstrated in the bottom row of Figure 10 where the v_2 and v_3 anisotropies are scaled by the respective number of constituent quarks (n_q) and displayed as a function of transverse kinetic energy (KE_T) per n_q. For similar event multiplicities the quark number scaling holds in Pb+Pb collisions only up to about 25% [63].

The strongest evidence for collective origin of long-range correlations in pseudorapidity in p+Pb collisions is provided by multiparticle correlations. The v_2 measurements based on two- and four-particle correlations are however known to suffer from contributions from effects such as fragmentation of back-to-back jets which mimic collective origin of the v_2 values. Therefore it is crucial to test the anticipated collective origin of the long-range correlations by measuring v_2 via six- and eight-particle cumulant methods as well as the Lee-Yang Zeros (LYZ) method that involves
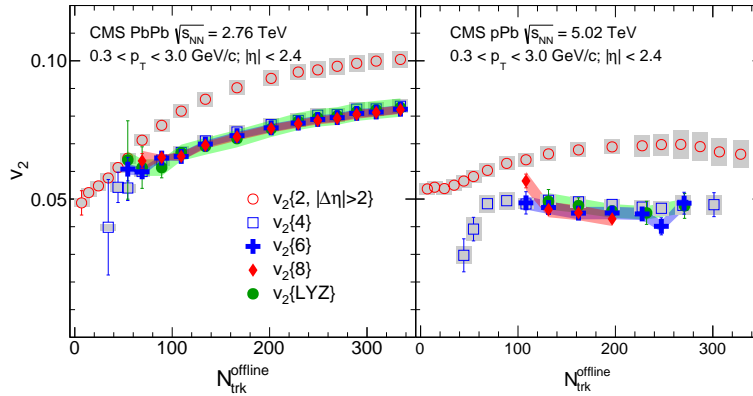
Figure 11: v_2 values extracted from different methods (see legend) as a function of multiplicity in Pb+Pb collisions at $\sqrt{s_{NN}} = 2.76$ TeV (left) and p+Pb collisions at $\sqrt{s_{NN}} = 5.02$ TeV (right) measured by CMS [64].
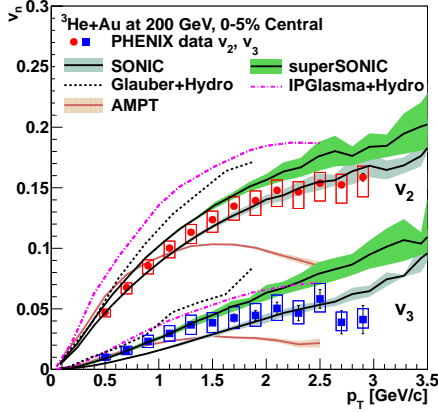
Figure 12: Elliptic (v_2, circles) and triangular (v_3, squares) anisotropies in central ^{3}He+Au collisions at $\sqrt{s_{NN}}$ = 200 GeV measured by the PHENIX experiment. The data are compared with several model calculations (see legend and text). Figure taken from [66].

correlations among all particles in an event. The CMS measurement of v_2 values obtained from six- and eight-particle correlations as well as the LYZ method is presented in Figure 11 for both Pb+Pb (left) and p+Pb collisions (right) at LHC energies from Run1 [62, 64]. The v_2 values, averaged over particle p_T in the range of 0.3–3.0 GeV/c, are displayed as a function of event multiplicity and are compared with earlier measurements of two- and four-particle correlations [65]. While clearly the v_2 data from two-particle correlations show the bias from "non-flow" effects, the v_2 data from six- and more particle correlations are within uncertainties consistent with previously published four-particle results. This finding thus clearly supports the collective origin of the long-range pseudorapidity correlations in p+Pb collisions and provides strong constraints on models.

Last but not least, long-range correlations and large v_2 and v_3 anisotropies were also recently detected in ^{3}He+Au collisions at RHIC by the PHENIX experiment [66] and are shown in Figure 12. The data are compared with several models and clearly show that formation of small QGP droplets followed by their hydrodynamical expansion is offering an alternative explanation to glasma models which incorporate novel initial state effects. RHIC due to its versatility of collision systems offers therefore a large unexplored territory which will allow to choose the size and shape of the initial collision zone using various nuclei species in asymmetric collisions.

6. Summary

Studies of nuclear matter created in heavy-ion collisions at ultrarelativistic energies offer a unique place to probe the QCD phase diagram and non-abelian quantum field theory (QCD) in laboratory. Run1 at the LHC at CERN as well as recent high statistics data from RHIC experiments brought rich collection of new physics results and important insights on jet production and particle correlations in hot and dense QCD matter as well as novel features in particle production in 'cold' nuclear matter created in small collision systems such as p+Pb, d+Au, ^{3}He+Au or high-multiplicity pp collisions. The initial measurements moved from inclusive jet measurements and dihadron correlations to more differential observables including correlated jet production, hadron-jet correlations, particle identification in jets or multiparticle correlations which will enable to constrain details of jet quenching mechanism, collective effects on particle production and hadronization mechanisms.

Run2 at the LHC will bring yet more statistics and also experiments at RHIC will collect and analyze high statistics data with upgraded detectors which will open new avenues in research of jets and correlations. These advances will enable to explore in detail for example jet shapes and extend particle identified jet studies to heavy-flavour sector. Last but not least we would like to mention that for the future of heavy-ion physics it is absolutely crucial to maintain both RHIC and LHC heavy-ion programmes operational as the complementarity of both colliders and all experiments operating at the LHC and RHIC is inevitable to pin down elusive characteristics of QGP and the QCD phase diagram in general.

7. Acknowledgments

References

[1] R. Granier de Cassagnac, *Heavy flavour production in heavy-ion collisions*, these proceedings.

[2] STAR Collaboration, C. Adler *et al.*, Phys. Rev. Lett. **89**, 202301 (2002).

[3] STAR Collaboration, J. Adams *et al.*, Phys. Rev. Lett. **91**, 172302 and 072304 (2003).

[4] STAR Collaboration, B.I. Abelev *et al.*, Phys. Rev. Lett. **98**, 192301 (2007).

[5] STAR Collaboration, C. Adler *et al.*, Phys. Rev. Lett. **90**, 82302 (2003).

[6] STAR Collaboration, J. Adams *et al.*, Phys. Rev. Lett. **95**, 152301 (2005).

[7] PHOBOS Collaboration, B. Alver *et al.*, Phys. Rev. Lett. **104**, 062301 (2010).

[8] STAR Collaboration, B. I. Abelev *et al.*, Phys. Rev. **C80**, 064912 (2009).

[9] STAR Collaboration, M. Ploskon *et al.*, Nucl.Phys. **A830**, 255C (2009).

[10] STAR Collaboration, E. Bruna *et al.*, Nucl.Phys. **A830**, 267C (2009).

[11] ATLAS Collaboration, Phys. Lett. **B739** 320 (2014).

[12] CMS Collaboration, Phys. Rev. **C90** 024908 (2014).

[13] ALICE Collaboration, J. Adam *et al.*, Phys. Lett. **B746** 1 (2015).

[14] ATLAS Collaboration, G. Aad *et al.*, Phys. Rev. Lett. **114** 072302 (2015).

[15] ATLAS Collaboration, G. Aad *et al.*, Phys. Rev. Lett. **105**, 252303 (2010).

[16] CMS Collaboration, S. Chatrchyan *et al.*, Phys.Rev. **C84**, 024906 (2011).

[17] ATLAS Collaboration, G. Aad *et al.*, Phys. Rev. Lett. **111** 152301 (2013).

[18] CMS Collaboration, Y.-S. Lai *et al.*, these proceedings and CMS-PAS-HIN-14-010.

[19] ATLAS Collaboration, D. Perepelitsa *et al.*, these proceedings and ATLAS-CONF-2015-021.

[20] ALICE Collaboration, J. Adam *et al.*, arXiv:1509.07334.

[21] ATLAS Collaboration, G. Aad *et al.*, Phys.Lett. **B751**, 376 (2015).

[22] ALICE Collaboration, J. Adam *et al.*, JHEP **09**, 170 (2015), 1506.03984.

[23] STAR Collaboration, A. Schmah *et al.*, Hard Probes 2015 Conference, http://www.physics.mcgill.ca/hp2015/.

[24] STAR Collaboration, J. Rusnak *et al.*, these proceedings, PoS(EPS-HEP2015)207.

[25] G. D'Agostini, Nucl. Instrum. Meth. **A 362**, 487 (1995).

[26] A. Hocker, V. Kartvelishvili, Nucl. Instrum. Meth. **A 372**, 469 (1996), hep-ph/9509307.

[27] CMS Collaboration, S. Chatrchyan *et al.*, Phys.Lett. **B718** 773 (2013).

[28] STAR Collaboration, B. I. Abelev *et al.*, Phys. Rev. Lett. **97**, 152301 (2006).

[29] STAR Collaboration, M. A. C. Lamont *et al.*, J.Phys. **G30** S963-S968 (2004).

[30] STAR Collaboration, J. Adams *et al.*, http://arxiv.org/abs/nucl-ex/0601042.

[31] ALICE Collaboration, B. I. Abelev *et al.*, Phys. Rev. Lett. **111** 222301 (2013).

[32] ALICE Collaboration, B. I. Abelev *et al.*, Phys. Lett. **B 728** 25 (2014).

[33] R. J. Fries, V. Greco, and P. Sorensen, Ann. Rev. Nucl. Part. Sci. 58 177 (2008).

[34] R. C. Hwa, C. B. Yang, Phys. Rev. **C70** 024905 (2004).

[35] R. C. Hwa, L. Zhu, Phys. Rev. **C84** 064914 (2011).

[36] K. Werner, Phys. Rev. Lett. **109** 102301 (2012).

[37] C. Shen, U. Heinz, P. Huovinen, and H. Song, Phys. Rev. **C84** 044903 (2011).

[38] ALICE Collaboration, X. Zhang *et al.*, XXIV Quark Matter 2014 conference, Germany, https://indico.cern.ch/event/219436/session/15/contribution/427

[39] ALICE Collaboration, V. Kucera *et al.*, 7th International Conference on Hard and Electromagnetic Probes of High-Energy Nuclear Collisions (Hard Probes 2015), Canada, arXiv: 1511.02766.

[40] CMS Collaboration, S. Chatrchyan *et al.*, JHEP **1107** 076 (2011).

[41] ALICE Collaboration, K. Aamodt *et al.*, Phys.Lett. **B708** 249 (2012).

[42] ATLAS Collaboration, G. Aad *et al.*, Phys. Rev. **C86**, 014907 (2012).

[43] P. Bozek, Phys. Rev. **C85** 014911 (2012).

[44] P. Bozek, W. Broniowski, Phys. Lett. **B718** 1557 (2013).

[45] K. Dusling, R. Venugopalan, Phys. Rev. **D87**, 054014 and 051502 (2013).

[46] CMS Collaboration, V. Khachatryan *et al.*, JHEP **1009**, 091 (2010).

[47] CMS Collaboration, S. Chatrchyan *et al.*, Phys. Lett. **B718**, 795 (2013).

[48] ALICE Collaboration, B. Abelev *et al.*, Phys. Lett. **B719** 29 (2013).

[49] ATLAS Collaboration, G. Aad *et al.*, Phys. Rev. Lett. **110** 182302 (2013).

[50] ATLAS Collaboration, G. Aad *et al.*, arXiv:1509.04776

[51] CMS Collaboration, Marco Meissner *et al.*, these proceedings, LHCB-CONF-2015-004.

[52] ALICE Collaboration, J. Adam *et al.*, Phys. Lett. **B753** 126 (2016), arXiv: 1506.08032

[53] Z.-W. Lin, C. M. Ko, B.-A. Li, B. Zhang, and S. Pal, Phys. Rev. **C72** 064901 (2005).

[54] P. Huovinen *et al.*, Phys. Lett. **B503** 58 (2001).

[55] STAR Collaboration, C. Adler *et al.*, Phys. Rev. Lett. **87**, 182301 (2001).

[56] PHENIX Collaboration, S. S. Adler *et al.*, Phys. Rev. Lett. **91**, 182301 (2003).

[57] ALICE Collaboration, B. I. Abelev *et al.*, JHEP **1506** 190 (2015).

[58] ALICE Collaboration, B. Abelev *et al.*, Phys. Lett. **B 726**, 164 (2013).

[59] PHENIX Collaboration, A. Adare *et al.*, arXiv:1404.7461

[60] P.Bozek, W. Broniowski, G. Torrieri, Phys. Rev. Lett. **111** 172303 (2013).

[61] K. Werner, M. Bleicher, B. Guiot, I. Karpenko, T. Pierog, Phys. Rev. Lett. **112** 232301 (2014).

[62] CMS Collaboration, D. Devetak *et al.*, these proceedings, PoS(EPS-HEP2015)194.

[63] CMS Collaboration, V. Khachatryan *et al.*, Phys.Lett. **B 742**, 200 (2015).

[64] CMS Collaboration, V. Khachatryan *et al.*, Phys. Rev. Lett. **115**, 012301 (2015).

[65] CMS Collaboration, Phys. Lett. **B 724**, 213 (2013).

[66] PHENIX Collaboration, A. Adare *et al.*, Phys. Rev. Lett. **115**, 142301 (2015).

[67] E. Avsar, C. Flensburg, Y. Hatta, J.-Y. Ollitrault, T. Ueda, Phys. Lett. **B702** 394 (2011).

[68] K. Werner, I. Karpenko, T. Pierog, Phys. Rev. Lett. **106** 122204 (2011).

[69] W.-T. Deng, Z. Xu, C. Greiner, Phys. Lett. **B711** 301 (2012).

[70] B. Arbuzov, E. Boos, V. Savrin, Eur. Phys. J. **C71** 1730 (2011).

[71] C. Y. Wong, Phys. Rev. **C84** 024901 (2011).

[72] M. Strikman, Acta Phys. Polon. **B42** 2607 (2011).